Polyhedron 68 (2014) 172–179

Contents lists available at ScienceDirect

Polyhedron

journal homepage: www.elsevier.com/locate/poly

μ-Oxamido binuclear copper (II) complexes: Synthesis, crystal structure, DNA interaction and antibacterial studies

P.R. Chetana [a,*], Ramakrishna Rao [a], Debojyoti Lahiri [b], R.S. Policegoudra [c], Ravish Sankolli [d], M.S. Aradhya [e]

[a] Department of Chemistry, Bangalore University, Central College Campus, Bangalore 560001, India
[b] Department of Inorganic & Physical Chemistry, Indian Institute of Science, Bangalore 560012, India
[c] Department of Biotechnology, Defence Research Laboratory, Tezpur 784001, India
[d] Department of Solid State and Structural Chemistry Unit, Indian Institute of Science, Bangalore 560012, India
[e] Department of Fruit and Vegetable Technology, CFTRI, Mysore 570020, India

ARTICLE INFO

Article history:
Received 30 January 2013
Accepted 23 October 2013
Available online 1 November 2013

Keywords:
Binuclear
Copper (II)
Oxpn
DNA interaction
Antibacterial

ABSTRACT

Four binuclear copper (II) complexes $[Cu(oxpn)Cu(B)]^{2+}$ (**2**–**5**) bridged by N, N′-bis[3-(methylamino) propyl] oxamide (oxpn), where, B is N, N-donor heterocyclic bases (*viz.* 2,2′-bipyridine (bpy, **2**), 1,10-phenathroline (phen, **3**), dipyrido[3,2-d:2′,3′-f]quinoxaline (dpq, **4**) and dipyrido[3,2-a:2′,3′-c]phenazine (dppz, **5**) are synthesized, characterized by different spectroscopic and single crystal X-ray data technique. The phen (**3**) and dpq (**4**) complexes were structurally characterized by X-ray data analysis. Their DNA binding, oxidative cleavage and antibactirial activities were studied. The dpq (**4**) and dppz (**5**) complexes are avid binders to the Calf thymus DNA (CT-DNA). The phen (**3**), dpq (**4**) and dppz (**5**) complexes show efficient oxidative cleavage of supercoiled DNA (SC DNA) through hydroxyl radical (·OH) pathway in the presence of Mercaptopropionic acid (MPA).

1. Introduction

Recent progress in structure-based design of molecules targeted towards DNA cleavage show that the promise of this area as a source of novel therapeutic agents and continued as a vibrant area of research. Substantial progress has been made over the past couple of decades in the fundamental characterization of a variety of drug-DNA interactions [1–10]. The interaction of transition metal complexes with dioxygen in the presence of a reducing or oxidizing agent generates reactive oxygen species (ROS) that ultimately cleave DNA [7]. Oxidative DNA cleavage by redox-active metal complexes like $[Fe(edta)]^{2-}$ or $Cu(1,10\text{-phenanthroline})_2Cl_2$ is mediated by the production of reactive oxygen species, like $HO^{\bullet}$ through a Fenton-type mechanism [10]. These free radicals abstract the most accessible and exposed sugar hydrogen's and initiate the oxidative cleavage, leading to DNA scision.

Binuclear copper complexes are attracting much attention [11], because of their spin–spin coupling, selective binding to particular conformations of nucleic acid and efficient intramolecular activation of bound O_2 in DNA cleavage [12,13]. Incorporation of two or more Cu(II) centers in a single compound produces enhanced electrostatic interactions to the anionic DNA phosphate backbone and facilitates its binding to DNA [14]. The Cu(II) centers in close proximity may undergo multielectron reductive cleavage of O_2 to generate an equivalent amount of hydroxyl radicals ($HO^{\cdot}$) [15]. These features were excellently demonstrated by examples reported by Karlin et al., using polynuclear Cu(II) complexes [14,16,17]. Binuclear metal complexes with extended bridged structures exhibit spin exchange and charge transfer between metal ions [18–21], when such coordination complexes contains DNA-binding moiety that binds either at a groove, or as an intercalator, increases the DNA-targeting ability of the compound. Many metalloproteins and enzymes have multi-metal sites, which are essential for their biological and catalytic function. Few reports have been published which are devoted only to the synthesis of oxamido binuclear metal complexes [22] and no reports with DNA interaction studies of oxamido metal complexes.

An enzyme Catechol oxidases contain two Cu centers in their active site, catalyzes the two-electron oxidation of a broad range of *o*-diphenols (catechols). In sweet potato, two cupric ions of catechol oxidase bridged by hydroxo ligand [23]. The development of synthetic analogues of metalloenzymes containing dinuclear Cu centers has become an attractive approach to understand the mechanisms involved in bio-catalytic pathways. The present work stems from our interest to design and develop 3d-metal complexes that could cleave DNA in an oxygen independent pathway [29–31].

Herein, we report the syntheses, structure, DNA binding, oxidative DNA cleavage activity and antimicrobial activity of μ-oxamido ternary copper (II) complexes *i.e.* $[Cu(oxpn)(B)]^{+}$ (**1**–**5**) where B is

* Corresponding author. Fax: +91 80 22961353.
E-mail address: pr.chetana@gmail.com (P.R. Chetana).

0277-5387/$ - see front matter © 2013 Elsevier Ltd. All rights reserved.
http://dx.doi.org/10.1016/j.poly.2013.10.025

N,N-donor heterocyclic base, *viz.* bpy (**2**), phen (**3**), dpq (**4**) and dppz (**5**). The phen (**3**) and dpq (**4**) complexes have been structurally characterized by single crystal X-ray data. Studies have been made to explore the role of DNA binder and oxpn along with mechanistic pathway involved in the 'chemical nuclease' activity.

2. Experimental

2.1. Materials

All chemicals and reagents were obtained from commercial sources and were used without further purification. Solvents used for electrochemical and spectroscopic studies were purified by standard procedures [24]. The supercoiled pUC19 DNA (CsCl purified) was purchased from Bangalore Genei (India). Calf thymus (CT) DNA, Agarose (molecular biology grade), Distamycin-A, Catalase, Superoxide dismutase (SOD), Mercaptopropionic acid (MPA) and Ethidium bromide (EB) were obtained from Sigma (USA). Tris (hydroxymethyl) aminomethane-HCl (Tris–HCl) buffer solution was prepared by using deionized, sonicated triple distilled water. The N, N-donor heterocyclic base dipyrido[3,2-d:2′,3′-f]quinoxaline (dpq) and dipyrido[3,2-a:2′,3′-c]phenazene (dppz) ligands were prepared by literature procedure using 1,10-phenanthroline-5, 6-dione as a precursor reacted with ethylenediamine and *o*-phenyl diamine [25].

2.2. Synthesis of Cu(oxpn (**1**), $[Cu_2(oxpn)_2(B)]^{n+}$ where B = bpy (**2**), phen (**3**), dpq (**4**), dppz (**5**)

A solution of 0.1 mol of diethyl oxalate in 20 ml ethanol was added dropwise to a solution of 0.3 mol of 1, 3-propylenediamine in 30 ml ethanol cooled by an ice bath. The resulting solution was refluxed for 1 h and then cooled down. A 0.75 mol $Cu(OH)_2$ suspended in 500 ml of water was added, which led to formation of a violet solution and a brown solid. Red single crystals of Cu(oxpn) were obtained after evaporation of the solvent, it is soluble in water and insoluble in alcohol [26].

A 100 ml aqueous solution of 216 mg (1 mM) of Cu(oxpn) were successively added to 10 ml of an aqueous solution containing 371 mg (1 mM) of copper (II) perchlorate hexahydrate and 10 ml of an aqueous solution containing 158 mg (1 mM) of bpy (**2**), 198 mg phen (**3**), 232 mg dpq (**4**) and 282 mg dppz (**5**), on slow evaporation yields dark brown crystals and finally dried over P_4O_{10} (Yield: ~75%).

Anal. Calc. for (**1**): $C_8H_{16}CuN_4O_2$(M.W. 263.5) C, 36.43; H, 6.07; N, 21.25. Found: C, 36.44; H, 6.08; N, 21.22. λ_{max}, nm (ε, $M^{-1}\,cm^{-1}$) in water/DMF(5%): 764 (24), 757 (240), 729 (25), 532 (68), 231 (1913). FT-IR, cm^{-1} (KBr disc): 3398w, 3191s, 3124s, 2906m, 2875m, 2842m, 1585vs, 1359s, 1190m, 1151m, 1047m, 952s, 826m, 717m, 443s, (s, strong; m, medium; w, weak; vs very strong).

Anal. Calc. for (**2**): $C_{18}H_{24}Cu_2N_6O_{10}Cl_2$ (M.W. 682.5) C, 31.67; H, 3.51; N, 12.31. Found: C, 31.65; H, 3.47; N, 12.28%. λ_{max}, nm (ε, $M^{-1}\,cm^{-1}$) in water/DMF(5%): 776 (3440), 764 (3462), 605 (314), 570 (36032), 550 (373), 534 (199), 377 (107), 359 (812), 291 (30207), 283 (11791). FT-IR, cm^{-1} (KBr disc): 3413m, 3326m, 3276m, 2925m, 1629s, 1448s, 1348w, 1313w, 1089vs, 933w, 779m, 730m, 626m, 437w. Λ_M ($\Omega^{-1}\,cm^2\,M^{-1}$) in DMF at 25 °C: 112.

Anal. Calc. for (**3**) $C_{40}H_{49}Cu_4N_{12}O_{22}Cl_4$ (M.W. 1444.6): C, 33.20; H, 3.39; N, 11.62. Found: C, 33.18; H, 3.44; N, 11.57%. λ_{max}, nm (ε, $M^{-1}\,cm^{-1}$) in water/DMF(5%): 626 (72), 602 (65), 376 (903), 232 (1356), 208 (1168), FT-IR, cm^{-1} (KBr disc): 3413m, 3265w, 2927w, 1629s, 1431m, 1344m, 1089vs (ClO_4^-), 931w, 858m, 723m, 626m, 437w. Λ_M ($\Omega^{-1}\,cm^2\,M^{-1}$) in water at 25 °C: 251.

Anal. Calc. for (**4**) $C_{22}H_{26}Cu_2N_8O_{11}Cl_2$ (M.W. 775.5): C, 34.04; H, 3.22; N, 14.44. Found: C, 34.07; H, 3.22; N, 14.42%. λ_{max}, nm (ε, $M^{-1}\,cm^{-1}$) in water/DMF(5%): 604 (55), 310 (13,420), 300 (13,620), 243 (10,220). FT-IR, cm^{-1} (KBr disc): 3429m, 2931m, 2854w, 1629s, 1446s, 1406m, 1346w, 1311w, 1087vs, 933w, 825w, 732w, 630s, 437 m. Λ_M ($\Omega^{-1}\,cm^2\,M^{-1}$) in DMF at 25 °C: 109.

Anal. Calc. for (**5**) $C_{26}H_{27}Cu_2N_8O_{11}Cl_2$ (M.W. 825.5): C, 37.79; H, 3.22; N, 14.44. Found: C, 37.43; H, 3.33; N, 14.43%. λ_{max}, nm (ε, $M^{-1}\,cm^{-1}$) in water: 611 (55), 293 (8,320), 272 (27,620), 204 (38,660). FT-IR, cm^{-1} (KBr disc): 3434m, 3276w, 3236w, 3139w, 2933m, 1629vs, 1444s, 1402m, 1087vs, 831m, 734m, 626m, 547w, 437m. Λ_M ($\Omega^{-1}\,cm^2\,M^{-1}$) in DMF at 25 °C: 118.

2.3. General methods

The elemental analysis was done using a Thermo Finnigan FLASH EA 1112 CHNS analyzer. The infrared and electronic spectra were recorded on Perkin Elmer spectrum one 55 spectrophotometers and Perkin Elmer Lambda 35 respectively. DNA melting experiments were carried out on a Varian Cary 300 Bio UV–Vis spectrophotometer attached to a Cary Peltier temperature controller. Molar conductivity measurements were done using a Control Dynamics (India) conductivity meter. Electrochemical measurements were made at 25 °C on an EG&G PAR model 253 VersaStat potentiostat/galvanostat with electrochemical analysis software 270 using a three electrode setup consisting of a glassy carbon working, platinum wire auxiliary and a saturated calomel reference electrode (SCE) in DMF containing 0.1 M Tetrabutylammonium perchlorate (TBAP). The electrochemical data were uncorrected for junction potentials.

2.4. X-ray crystallographic procedures

Single crystals of complex **3** and **4** were obtained by slow evaporation of the aqueous-methanolic solution of the complexes. A rectangular single crystal was mounted on a glass fiber and used for data collection. All geometric and intensity data were collected at 293 K using an automated Bruker SMART APEX CCD diffractometer equipped with a fine focus 1.75 kW sealed tube Mo Kα X-ray source (λ = 0.71073 Å), with increasing ω (width of 0.3°/frame) at a scan speed of 5 and 2 s/frame for complex **3** and **4** respectively. Intensity data, collected using ω – 2θ scan mode, were corrected for Lorentz-polarization effects and for absorption [27]. The SMART software was used for data acquisition and the SAINT software for data extraction [28]. Absorption corrections were made using SADABS [29]. The structure was solved and refined by full-matrix least-squares method using SHELX system of programs [30]. All non-hydrogen atoms were refined anisotropically. All hydrogen atoms attached to the heteroatoms were in their calculated positions and refined using a riding model. Perspective views of the complexes were obtained by ORTEP [31]. CCDC reference numbers 806157 and 806156 for complex **3** and **4** respectively.

2.5. DNA binding experiments

In the UV–visible absorption titration experiments, absorbance at 260 and 280 nm for CT-DNA in 5 mM Tris–HCl buffer (pH 7.2) gave a ratio of 1.9:1, indicating the DNA free of protein [32]. The concentration of CT-DNA was measured from the band intensity at 260 nm with a known ε value (6600 $M^{-1}\,cm^{-1}$) [33]. Absorption titration measurements were done by varying the concentration of CT-DNA keeping the complex concentration(40 μM) constant in 5 mM Tris–HCl/5 mM NaCl buffer (pH 7.2). The intensity of the band at ~260 nm was monitored for the complexes. Correction was made for the absorption of DNA itself. The spectra were recorded after equilibration for 5 min, allowing the complexes to

bind to the DNA. The intrinsic equilibrium DNA binding constant (K_b) values of the complexes to CT-DNA were obtained by McGhee–von Hippel (MvH) method using the expression of Bard and coworkers by monitoring the change in the absorption intensity [34].

The apparent binding constant (K_{app}) values of the complexes were determined by fluorescence spectral technique using EB bound CT-DNA solution in Tris–HCl/NaCl buffer (pH, 7.2). The emission intensities of EB at 600 nm (546 nm excitation) with an increasing amount of the complex concentration were recorded. The K_{app} values were obtained from equation: $K_{app}[complex]_{50} = K_{EB}[EB]$, where, K_{app} is the apparent binding constant of the complex studied, $[complex]_{50}$ is the concentration of the complex at 50% quenching of DNA bound EB emission intensity, K_{EB} is the binding constant of EB($K_{EB} = 1.0 \times 10^7\ M^{-1}$) and [EB] is the concentration of ethidium bromide (1.3 M). EB was non-emissive in Tris-buffer medium due to fluorescence quenching of the free EB by the solvent molecules [35]. In the presence of DNA, EB showed enhanced emission intensity due to its intercalative binding to DNA. A competitive binding of the coper complexes to CT-DNA could result in the displacement of EB or quenching of the bound EB by the paramagnetic copper (II) species decreasing its emission intensity.

DNA-melting experiments were carried out by monitoring the absorbance of CT-DNA (200 μM nucleobase pair (NP) at 260 nm with varying temperature in the absence and presence of the complexes in a 2:1 ratio of DNA–Complex with a ramp rate of 0.5 °C min^{-1} in phosphate buffer (pH 6.85) using a Peltier system attached to the UV–Vis spectrophotometer.

Viscometric titrations were performed with a Schott Gerate AVS 310 Automated Viscometer. The viscometer was thermostated at 37 °C in a constant temperature bath. The concentration of DNA was 200 M in nucleobase pair (NP) and the flow times were measured with an automated timer and each sample was measured 3 times and an average flow time was calculated. Data were presented as $(\eta/\eta_0)^{1/3}$ vs. [complex]/[DNA], where η is the viscosity of DNA in the presence of complex and $_0$ that of DNA alone. Viscosity values were calculated from the observed flowing time of DNA-containing solutions (t) corrected for that of buffer alone (t_0), $\eta = (t - t_0)$ [36].

2.6. DNA cleavage experiments

The extent of cleavage of supercoiled (SC) DNA in the presence of the complex and reducing agent MPA was determined by agarose gel electrophoresis. In a typical reaction, supercoiled pUC19 DNA (0.2 μg), taken in 50 mM Tris–HCl buffer (pH 7.2) containing 50 mM NaCl, was treated with the complex. The extent of cleavage was measured from the intensities of the bands using UVITEC Gel Documentation System.

For mechanistic investigations, inhibition reactions were done on adding the reagents prior to the addition of the complex. The solutions were incubated for 1 h in a dark chamber at 37 °C followed by addition of the loading buffer containing 0.25% bromophenol blue, 0.25% xylene cyanol and 30% glycerol (2 μL) and the solution was finally loaded on 1.0% agarose gel containing 1.0 μg/ml EB. Electrophoresis was carried out for 2 h at 60 V in tris–acetate-EDTA (TAE) buffer. Bands were visualized by UV light and photographed for analysis. Due corrections were made to the observed intensities for the low level of NC form present in the original sample of SC DNA and for the low affinity of EB binding to SC in comparison to nicked circular (NC) and linear forms of DNA [37]. The concentration of the complexes or the additives mentioned corresponded to the quantity of the sample in 2 μL stock solution prior to dilution to the 20 μL final volume by Tris–HCl buffer.

2.7. Antimicrobial activity

The antibacterial activity was tested against clinical isolates like *B. subtilis, Micrococcus luteus*, *Staphylococcus aureus*, *Staphylococcus mutans*, *Escherichia coli*, *Pseudomonas aeruginosa* and *Proteus vulgaris*. The test organisms were maintained on nutrient agar slants. *In vitro* antibacterial activity was determined by the agar well-diffusion method as described by Mukherjee et al. [38]. The overnight bacterial culture was centrifuged at 8000 rpm for 10 min. The bacterial cells were suspended in saline to make a suspension of 105 CFU/mL and used for assay. Plating was carried out by transferring the bacterial suspension to a sterile Petri plate, mixed with molten nutrient agar medium and allowed to solidify. About 75 μL of the sample (2 mg/mL) was placed in the wells. Plates were incubated at 37 °C and activity was determined by measuring the diameter of the inhibition zones. The assay was carried out in triplicate. The minimum inhibitory concentration (MIC) values were determined according to the method described by Jones et al. [39].

Different concentrations of the compounds and 100 μl of the bacterial suspension (105 Colony-forming unit (CFU)/mL)) were placed aseptically in 10 ml of nutrient broth separately and incubated for 24 h at 37 °C. Growth was observed at regular intervals followed by pour plating as described above. The lowest concentration of the test sample showing no visible growth was recorded as the MIC. Triplicate sets of tubes were maintained for each concentration of test sample.

3. Results and discussion

3.1. Synthesis and general aspects

The binuclear copper (II) complexes were prepared in high yield from the reaction of Cu(oxpn) and $Cu(ClO_4)_2{\cdot}7H_2O$ with heterocyclic bases. The complexes are stable and soluble in common polar organic solvents. They are characterized from the analytical and physicochemical data (Table 1, Scheme 1). The complexes display intense charge transfer band in the range of 200–310 nm that can be attributed to the $\pi \rightarrow \pi^*$ transition of the coordinated *N*, *N*-donor heterocyclic base. The d–d band is observed at ~600 nm in an aqueous medium (Fig. 1). All the complexes exhibit strong absorption peak between 200–275 cm^{-1} attributable to plane ring vibrations. The bands between 300–400 cm^{-1} may be assigned to ring and metal–nitrogen vibrations. All the complexes are showing a characteristic perchlorate peak at 1087–1089 cm^{-1} (ν_{ClO4}). The coordinated perchlorate shoulder peaks appear at 1035, 1143 cm^{-1} on either sides of characteristic perchlorate peak (Figs. S1, S2). Complexes **1**–**5** are redox active showing cyclic voltammetric responses involving the metal center and the ligands in DMF-0.1 M TBAP (Table 1, Fig. S3). Anodic response (E_{pa}) is observed near 0.540 V and with cathodic counterpart (E_{pc}) at ca. −0.589 V. The anodic response is assigned to the Cu(II)/Cu(I) redox couple showing a i_{pc}/i_{pa} peak current ratio of ~0.904 (i_{pc}, i_{pa} are cathodic and anodic peak currents, respectively). Copper (II) complexes having readily accessible metal-based Cu(II)/Cu(I) redox couple show significant "chemical nuclease" activity in the presence of reducing thiols [40].

3.2. Crystal structures

The phen and dpq complexes (**3** and **4**) are structurally characterized using single-crystal X-ray diffraction technique. Selected crystallographic data are summarized in Table 2. The selected bond distances and angles present in **3** and **4** are shown in Table 3. ORTEP views of **3** and **4** are shown in Figs. 2 and 3 respectively. The **3** crystallizes in the monoclinic space group *P*21/*c*. In two different

Table 1
Physicochemical data for the ternary copper (II) complexes **1–5**.

Complex	1	2	3	4	5
IR[a]: [ν/cm^{-1}](ClO_4^-)	–	1089	1089	1089	1087
$\gamma_{(C{=}O)}$	1583	1629	1629	1629	1629
d–d band: λ_{max}/nm (ε/M^{-1} cm^{-1})[b]	538 (46)	605 (314)	602 (65)	541 (55)	583 (55)
CV: $E_{1/2}$/V(ΔE_p/mV)[c]	0.113 (1092)	−0.034 (1126)	−0.09 (1498)	−0.025 (981)	−0.55 (1096)
Λ_M[d] (Ω^{-1} cm^2 M^{-1})	–	112 (in DMF)	251 (in water)	109 (in DMF)	118 (in DMF)
Isosbestic (nm) Point	213, 274	–	243	247	–
$_a$[e] (M^{-1})	2.51×10^5	3.5×10^6	5.5×10^6	7.86×10^6	9.76×10^6
K_b[f] (M^{-1})	–	5.1×10^3 (±0.3)	1.14×10^5 (±0.2)	8.78×10^5 (±0.1)	2.24×10^6 (±0.3)
ΔT_m[g] (°C)	0.5 (0.2)	0.8 (0.2)	1.4 (0.2)	1.8 (0.3)	2.4 (0.2)

[a] KBr phase.
[b] In aqueous medium.
[c] Cu(II)/Cu(I) couple in DMF-0.1 M TBAP. $E_{1/2} = 0.5(E_{pa} + E_{pc})$, $\Delta E_p = |E_{pa} - E_{pc}|$, where E_{pa} and E_{pc} are the anodic and cathodic peak potentials, respectively. Scan rate: 50 mV s^{-1}.
[d] In aqueous/DMF medium at 25 °C.
[e] Apparent DNA binding constant from competitive binding assay by emission method.
[f] Intrinsic DNA binding constant (K_b) from absorption spectral method.
[g] Changes in melting temperature of CT DNA.

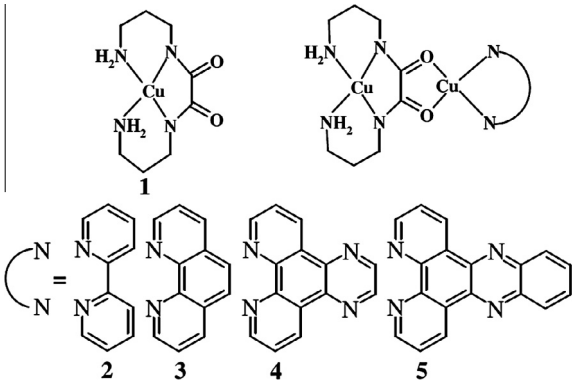

Scheme 1. Structures of the ternary copper (II) complexes (**1–5**) and phenanthroline bases.

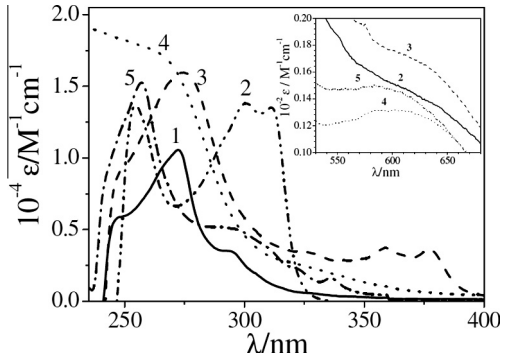

Fig. 1. Electronic spectra of complexes **1–5** and the inset shows the d–d band of the complexes.

molecules, four metal centers with coordination environment around the Cu were $N_4O_1 + N_2O_2$ and $N_2O_3 + N_4O_1$. The **4** crystallizes in the monoclinic space group $P2_1/n$. It shows distorted square-pyramidal (4 + 1) coordination (CuN_4O and CuN_2O_3) geometry with weakly coordinated apical perchlorate anions at both metal centers. The Cu1–Cu2 separation within the binuclear cation is 5.196(1) Å. Average trigonal distortion parameter at Cu1 and Cu2 are 0.069 and 0.033 Å, respectively.

Both **3** and **4** show extensive intermolecular non-covalent interactions. The unit cell packing diagrams and intermolecular hydrogen bonding interactions present in **3** and **4** are shown in Figs. S4–S7 (see Supporting information).

3.3. DNA binding properties

Absorption titration technique has been used to monitor the mode of interaction of the complexes **1–5**.

Changes in the $\pi \rightarrow \pi^*$ transition of **1–5** in DMF/5 mM Tris–HCl/50 mM NaCl buffer at pH 7.1 were determined as a function of increased DNA concentration and the typical titration curve for **4** is shown in Fig. 4. The intrinsic DNA binding constants (K_b) of the complexes to CT-DNA are obtained by monitoring the change of the absorption intensity of the spectral bands with increasing concentration of CT-DNA, keeping complex concentration constant. The intrinsic equilibrium DNA binding constant (K_b) values of the complexes are given in Table 1. The values of intrinsic binding constants K_b determined from these changes follow the order **5 > 4 > 3 > 2**. The dppz complexes show higher K_b values in comparison to their dpq and phen analogues possibly because of the presence of an extended planar aromatic moiety in dppz which facilitating non-covalent interactions with DNA. It primarily interacts with the ds-DNA via intercalation and gets additional stabilization by partial π-stacking interactions with the purine and pyrimidine DNA bases [41].

The hypochromism was suggested to be due to a strong interaction between the electronic states of the binding chromophore and that of the DNA bases [42–45]. An isosbestic point at 243 nm were also observed indicating one mode of binding with equilibrium between two species [44]. Complex **1** show two isosbestic points at 213 and 274 nm, suggesting mixed modes of DNA binding. The **3** show a single isosbestic point at 247 nm and **4** at 243 nm (Fig. S8).

We have used a fluorescence spectral titration method to obtain the apparent binding constant values (K_{app}). The emission intensity of EB is used as a spectral probe as EB shows no apparent mission intensity in buffer solution because of solvent quenching and an enhancement of the emission intensity when intercalatively bound to DNA [46]. The fluorescence intensities of EB at 600 nm (546 nm excitation) with an increasing amount of the ternary complex concentration were recorded. In the presence of DNA, EB showed enhanced emission intensity due to its intercalative binding to DNA. A competitive binding of the copper complexes to CT-DNA result in decrease of emission intensity. Relative binding propensity of the complexes to DNA is measured from the extent of reduction of the emission intensity (Fig. 5, Table 1).

The denaturation of DNA from double-strand to single strand results in absorption hyperchromism around 260 nm. The binding of metal complexes to the double-stranded DNA usually stabilizes the duplex structure to some extent depending on the strength of interaction with nucleic acid [47]. The binding should lead to an

Table 2
Selected main crystallographic data for 3 and 4.

	3	4
Empirical formula	$C_{40}H_{49}Cl_4Cu_4N_{12}O_{22}$	$C_{22}H_{25}Cl_2Cu_2N_8O_{11}$
Formula weight	1444.89	775.48
Crystal system	monoclinic	monoclinic
Space group	*P*21/*c*	*P*21/*n*
a (Å)	8.9133(2)	8.937(5)
b (Å)	24.4399(6)	11.986(5)
c (Å)	24.4409(5)	25.613(5)
β (°)	99.467(2)	93.123(5)
α = *γ* (°)	90	90
V (Å^3)	5251.7(2)	2740(2)
Z	4	4
T (K)	100(2)	100(2)
ρ_{calcd} (g cm^{-3})	1.829	1.883
λ Å (Mo Kα)	0.71073	0.71073
μ (cm^{-1})	1.894	1.825
Data/restraints/parameters	11418/0/407	5096/0/407
F(000)	2932	1598
Goodness-of-fit	1.084	1.057
R (F_o)[a], I > 2σ(I)/*wR* (F_o)[b]	0.0483/ 0.1225	0.0261/0.0666
R (all data)/*wR* (all data)	0.0677/ 0.1264	0.0313/0.0678
Largest difference in peak and hole (e Å^{-3})	1.270 and −0.831	0.611 and −0.371
$w = 1/[\sigma^2(F_o^2) + (AP)^2 + (BP)]$	A = 0.0503 B = 15.2520	A = 0.0354 B = 1.9640

[a] Denotes value of the residual considering only the reflections with I > 2σ(I).
[b] Denotes value of the residual considering all the reflections.

Table 3
Selected bond distances and bond angles present in **3** and **4.**

Complex **3**		Complex **4**	
Cu01–O1	1.938 (3)	Cu1–O1	2.583(2)
Cu01–O2	1.940 (3)	Cu1–N1	2.008(2)
Cu01–N2	1.985 (4)	Cu1–N2	2.010(2)
Cu01–N1	1.986 (4)	Cu1–N3	1.984(2)
Cu01–O3	2.314 (4)	Cu1–N4	1.981(2)
Cu02–N4	1.993 (4)	Cu2–O2A	2.417(2)
Cu02–N3	1.997 (4)	Cu2–O3	1.922(2)
Cu02–N5	2.016 (4)	Cu2–O4	1.944(2)
Cu02–N6	2.021 (4)	Cu2–N5	1.968(2)
Cu02–O4	2.416 (4)	Cu2–N6	1.995(2)
N4–Cu02–N3	82.94 (16)	N2–Cu1–N3	93.38(8)
N4–Cu02–O4	92.34 (15)	N2–Cu1–N4	176.55(8)
N3–Cu02–O4	97.21 (15)	N2–Cu1–O1B	85.95(7)
N5–Cu02–O4	85.92 (16)	N3–Cu1–N4	83.54(7)
N6–Cu02–O4	94.32 (16)	N4–Cu1–O1B	92.73(7)
N4–Cu02–N5	175.97 (17)	N1–Cu1–N3	172.41(8)
N3–Cu02–N5	93.67 (16)	N1–Cu1–N4	93.94(7)
N4–Cu02–N6	93.30 (16)	N1–Cu1–O1B	93.06(7)
N3–Cu02–N6	168.00 (18)	N3–Cu1–O1B	94.21(7)
N5–Cu02–N6	90.45 (16)	N5–Cu2–N6	83.01(7)
O1–Cu01–O2	86.28 (14)	O2A–Cu2–N5	88.27(6)
O1–Cu01–N2	95.40 (15)	O2A–Cu2–N6	89.17(6)
O2–Cu01–N2	168.35 (16)	O2A–Cu2–O3	98.01(6)
O1–Cu01–N1	174.31 (16)	O2A–Cu2–O4	99.16(6)
O2–Cu01–N1	93.80 (15)	O3–Cu2–N5	173.36(7)
N2–Cu01–N1	83.39 (16)	O3–Cu2–N6	94.85(7)
O1–Cu01–O3	93.65 (14)	O3–Cu2–O4	86.36(6)
O2–Cu01–O3	92.20 (14)	O4–Cu2–N5	94.82(7)
N2–Cu01–O3	99.18 (15)	O4–Cu2–N6	171.34(7)
N1–Cu01–O3	92.04 (15)		

increase in the melting temperature (T_m) of DNA as compared to DNA itself (Fig. 6(a), Table 1).

The DNA binding mode by the complexes was also studied by the viscometric titration method. Viscosity of a DNA solution is sensitive to the addition of compound which binds through by intercalation; we examined the effect on the specific relative viscosity of DNA upon addition of complexes, because the relative specific viscosity (/$_0$), (and $_0$ are the specific viscosities of DNA in

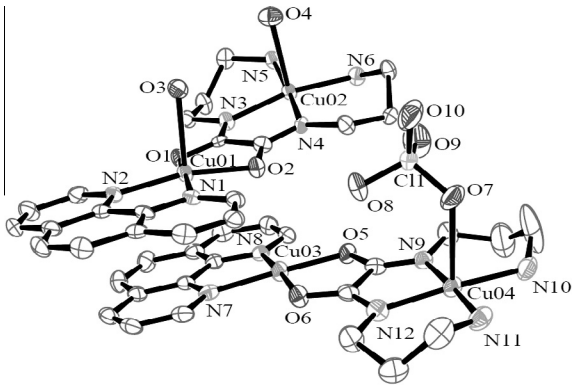

Fig. 2. ORTEP diagram of complex **3** showing 50% probability thermal ellipsoids with atom labeling scheme for metal and heteroatoms.

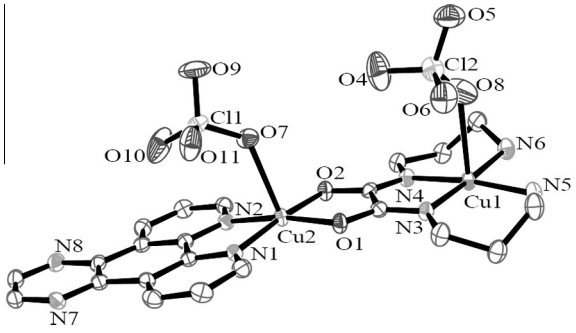

Fig. 3. ORTEP view of complex **4** showing 50% probability thermal ellipsoids with atom labeling scheme for the metal and heteroatoms.

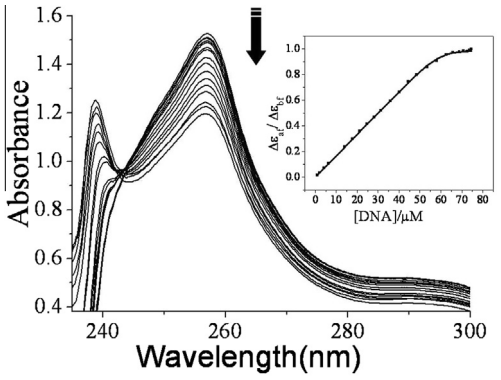

Fig. 4. (a) Absorption spectral traces on addition of CT-DNA to the solution of **4** (40 M) (shown by arrow). Inset shows plot of ($\Delta\varepsilon_{af} - \Delta\varepsilon_{bf}$) vs. [DNA] for absorption titration of CT-DNA with **4**.

the presence and absence of the complexes, respectively) of DNA reflects the increase in contour length associated with separation of DNA base pairs caused by complex binding. The relative viscosity of DNA and contour length follows the equation: (/$_0$) = (L/L_0)$^{1/3}$, where L and L_0 are the contour length of DNA in the presence and absence of the complexes respectively. A classical intercalator such as EB could cause a significant increase in viscosity of DNA solutions, in contrast, a partial and/or non-classical intercalation of the ligand could bend or kink DNA resulting in a decrease in its effective length with a concomitant increase in its viscosity [48]. The plots of relative viscosities with R = [Cu]/[DNA] are shown in Fig. 6(b). The change in relative viscosity of dppz complex is more

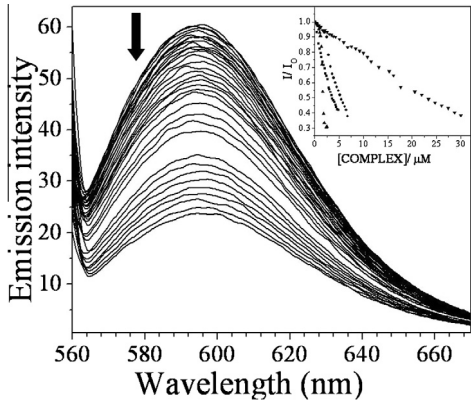

Fig. 5. Emission spectral changes on addition of **4** to the CT-DNA bound to ethidium bromide (shown by arrow). Inset: Effect of addition of metal complex [B = bpy **2** (▼); phen **3** (●); dpq **4** (■), dppz **5** (▲)] to the emission intensity CT-DNA-bound ethidium bromide in a 5 mM Tris–HCl/5 mM NaCl buffer (pH 7.2) at 25 °C.

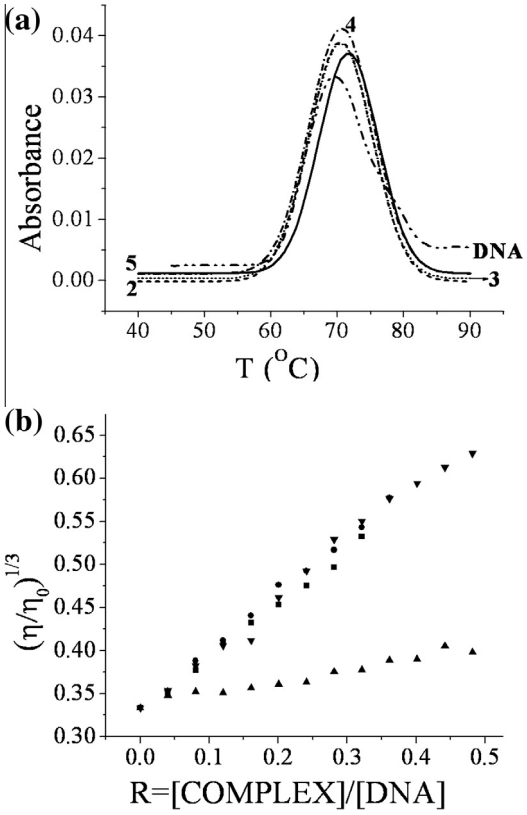

Fig. 6. (a) Effect of addition of complexes (**1**–**5**) (20 μM) on the melting temperature of CT-DNA (200 M) in 5 mM Phosphate buffer (pH 6.85) with a ramp rate of 0.5 °C/min. (b) Change in relative specific viscosity of CT-DNA (150 μM) with addition of complex bpy **2** (▲); phen **3** (●); dpq **4** (■), dppz **5** (▼)] in 5 mM Tris–HCl buffer medium at 37 ± 0.1 °C.

than the dpq, phen and bpy analogues suggesting high intercalative binding propensity of the dppz complexes in comparison to their analogues.

The DNA binding ability of copper complexes was essential to mediate DNA cleavage when DNA-bound ROS acted as the direct oxidative intermediates and higher DNA affinity normally leads to higher DNA cleavage efficiency [49]. Since polynuclear complexes can enhance the affinity to anionic DNA and enhance their

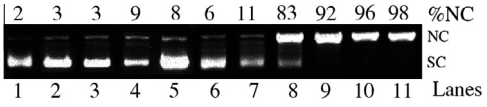

Fig. 7. Gel electrophoresis diagram showing the oxidative cleavage of SC pUC19 DNA (0.2 g), by the 10M complexes (**1**–**5**) in the presence of 500 M MPA in 50 mM Tris–HCl/NaCl buffer (pH, 7.2). lane-1, DNA control; lane-2, DNA + **1**; lane-3, DNA + **2**; lane-4, DNA + **3**; lane-5, DNA + **4**; lane-6, DNA + **5**; lane-7, DNA + **1** + MPA; lane-8, DNA + **2** + MPA; lane-9, DNA + **3** + MPA; lane-10, DNA + **4** + MPA; lane-11, DNA + **5** + MPA.

Table 4
Selected DNA cleavage data for complex **5**.

Lane No.	Condition	%NC
1	DNA control	2
2	DNA + MPA (200 mM)	3
3	DNA + **5** (10 μM)	6
4	DNA + MPA (200 mM) + **5** (10 μM)	98
5	DNA + MPA (200 mM) + NaN3 (500 μM) + **5** (10 μM)	89
6	DNA + MPA (200 μM) + TEMP (500 μM) + **5** (10 μM)	92
7	DNA + MPA (200 μM) + DABCO (500 μM) + **5** (10 μM)	97
8	DNA + MPA (200 μM) + KI (500 μM) + **5** (10μM)	32
9	DNA + MPA (200 μM) + DMSO (4 μL) + **5** (10μM)	57
10	DNA + MPA (200 μM) + D2O (14 μL) + **5** (10μM)	95
11	DNA + MPA (200 μM) + Catalase (4 units) + **5** (10μM)	42
12	DNA + MPA (200 μM) + SOD (4 units) + **5** (10μM)	90
13	DNA + MPA (200 μM) + distamycin (200 μM) + **5** (10 μM)	91
14	DNA + MPA (200 μM) + methyl green (200 μM) + **5** (10 μM)	34

Fig. 8. Mechanistic study of cleavage of SC pUC19 DNA (30 μM) by **5** in the presence of MPA (5 mM) with various additives in Tris buffer (pH 7.2) medium.

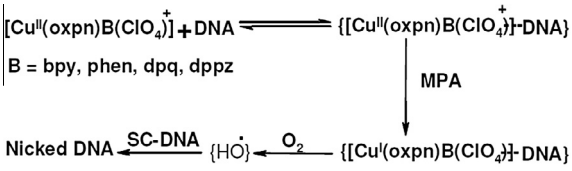

Scheme 2. Proposed mechanistic pathway for the chemical nuclease activity of complexes in Tris-buffer medium in presence of MPA.

DNA cleavage activity. The DNA binding affinity of the complexes showed the following order **5** > **4** > **3** > **2** > **1**. Phenanthroline and its derived ligands *viz*., dpq, dppz are sterically compact due to extended heterocyclic ring system and metal complexes with such ligands have relatively shielded surfaces and help towards DNA-complex non covalent binding [50,51].

3.4. DNA cleavage studies

The oxidative DNA cleavage activity of the complexes in the presence of reducing agent MPA (5 mM) is studied by agarose gel electrophoresis using supercoiled (SC) plasmid pUC19 DNA (0.2 g, 30 M NP) in 50 mM Tris–HCl/50 mM NaCl buffer (pH, 7.2) and the Copper (II) complexes (Fig. 7). Selected DNA cleavage data were given in Table 4. Cu^{2+}(aq) alone or with added MPA did not show DNA cleavage activity.

The phen, dpq and dppz complexes show significant "chemical nuclease" activity. A 10 μM complex **3**–**5** shows almost complete conversion of the SC (form I) to its nicked circular form (NC, form

Table 5
Minimum inhibitory concentration for complexes **1**–**5** and ligands (μg/mL).

Bacterial Strains	**1**	**2**	**3**	**4**	5	bpy	phen	Ampicillin*
Bacillus subtilis	–	>1000	–	350	450	–	450	16.0
Micrococcus luteus	–	1000	–	425	500	500	1000	11.7
Staphylococcus aureus	>1000	–	–	475	450	–	>1000	11.0
Streptococcus mutans		–	–	475	500	1000	>1000	19.8
E. coli	–	20	–	1000	1000	–	500	7.2
Pseudomonas aeruginosa	–	–	–	500	350	–	1000	18.7
Proteus vulgaris	–	–	–	350	400	–	1000	NT

* Positive control, NT – not tested.

II) of DNA. Mechanistic aspects of the chemical nuclease reactions are performed using various control experiments (Fig. 8). In absence of complex, MPA or the ternary complexes showed no apparent conversion of SC to its nicked-circular (NC) form. Complexes **5** displayed significant reduction in the chemical nuclease activity in the presence of methyl green, while similar inhibition for the complexes **2** and **3** was observed in the presence of distamycin-A [52]. Addition of hydroxyl radical scavengers [53] like DMSO, catalase, KI shows significant inhibition of the DNA cleavage activity (lane 8, 9 and 11; Fig. 8, Table 4) of the complexes indicating the possibility of the involvement of hydroxyl radical and/or "copper-oxo" intermediate as the reactive species. Addition of superoxide dismutase (SOD) or singlet oxygen scavengers (lane 5, 6 and 7) does not show any apparent effect on the DNA cleavage activity suggesting the non-involvement of $O_2^{\cdot -}$ or singlet oxygen in the cleavage reactions [54]. No considerable inhibition of DNA cleavage was observed in presence of sodium azide and as well as no enhancement of DNA cleavage in the presence of D_2O indicating the singlet oxygen were not a reactive species in the scission reactions (Scheme 2). MPA could form reduced Cu(I) species that can activate molecular oxygen to generate ·OH radical following a mechanistic pathway that is known for the chemical nuclease activity of bis-phen copper species [1,55].

4. Antimicrobial activity

The antimicrobial activity of the complexes **1**–**5** ligands and copper salt was evaluated against a panel of pathogenic bacterial strains by disc diffusion and serial dilution method in aqueous/DMF medium. The result obtained for zone inhibition exhibited by the complexes and the ligands are summarized in Table S1.

The **5** and **4** shows highest zone of inhibition against *B. subtilis*, *M. luteus*, *S. aureus*, *S. mutans*, *E. coli*, *P. aeruginos* and *P. vulgaris* respectively. **1** shows highest zone of inhibition 31 mm against *E. coli* compared with other complexes (Table S1). MIC values for complexes **1**–**5** and ligands are summarized in Table 5. The **2** shows highest antibacterial activity against *E. coli* with MIC value 20 μg/mL. The minimum inhibitory concentration values revealed that they have relatively better antibacterial activity compared to ligands. This might be due to reduction in the polarity of metal ion by partial sharing of its positive charge with the donor groups, increasing lipophilic nature of the central metal ion and in turn may favors its permeation to the lipid layer of the membrane. The complexes **1**–**5** and ligands were screened against fungus *Candida albica* observed no considerable activity under assay conditions.

5. Conclusion

Four binuclear copper (II) complexes $[Cu(oxpn)Cu(B)]^{2+}$ are synthesized, characterized and their DNA interactions were studied. The novel complexes labelled as **3** and **4** are structurally characterized by X-ray crystallography. The phen (**3**) complex crystallizes in the monoclinic space group $P21/c$. The dpq (**4**) complex crystallizes in the monoclinic space group $P2_1/n$. The results suggest that the dpq and dppz complexes are avid binders to the CT-DNA giving an order: (**5**) (dppz) > (**4**) (dpq) > (**3**) (phen) ≫ (**2**) (bpy) > (**1**). Binuclear copper (II) complexes having DNA binding phenanthroline bases and oxamide moiety show aerobic DNA cleavage activity in presence of MPA. Complexes do not cleave DNA under argon medium. The dppz complex due to its extended conjugated aromatic planar surface, shows highest DNA cleavage in presence of air and MPA, follows hydroxyl free radical pathway and major groove binding. 2 exhibited highest antibacteria activity against *E. coli* among the tested complexes.

Acknowledgements

The authors gratefully acknowledge the support of Prof. Akhil R. Chakravarty, Department of Inorganic and Physical Chemistry, Indian Institute of Science, Bangalore, India, in providing facilities and useful discussions.

Appendix A. Supplementary data

CCDC 806157 and 806156 contains the supplementary crystallographic data for **3** and **4**. These data can be obtained free of charge via http://www.ccdc.cam.ac.uk/conts/retrieving.html, or from the Cambridge Crystallographic Data Centre, 12 Union Road, Cambridge CB2 1EZ, UK; fax: (+44) 1223-336-033; or e-mail: deposit@ccdc.cam.ac.uk. Supplementary data associated with this article can be found, in the online version, at http://dx.doi.org/10.1016/j.poly.2013.10.025.

References

[1] (a) D.S. Sigman, A. Mazumder, D.M. Perrin, Chem. Rev. 93 (1993) 2295;
(b) D.S. Sigman, Acc. Chem. Res. 19 (1986) 180;
(c) K.A. Reich, L.E. Marshall, D.R. Graham, D.S. Sigman, J. Am. Chem. Soc. 103 (1981) 3582.
[2] (a) B. Meunier, Chem. Rev. 92 (1992) 1411;
(b) G. Pratviel, J. Bernadou, B. Meunier, Adv. Inorg. Chem. 45 (1998) 251;
(c) G. Pratviel, J. Bernadou, B. Meunier, Angew. Chem., Int. Ed. Engl. 34 (1995) 746.
[3] M. Pyle, J.K. Barton, Prog. Inorg. Chem. 38 (1990) 413.
[4] K.E. Erkkila, D.T. Odom, J.K. Barton, Chem. Rev. 99 (1999) 2777.
[5] B. Armitage, Chem. Rev. 98 (1998) 1171.
[6] (a) D.R. McMillin, K.M. McNett, Chem. Rev. 98 (1998) 1201;
(b) F. Mancin, P. Scrimin, P. Tecilla, U. Tonellato, Chem. Commun. (2005) 2540.
[7] (a) W.K. Pogozelski, T.D. Tullius, Chem. Rev. 98 (1998) 1089;
(b) T.D. Tullius, J.A. Greenbaum, Curr. Opin. Chem. Biol. 9 (2005) 127.
[8] H.T. Chifotides, K.R. Dunbar, Acc. Chem. Res. 38 (2005) 146.
[9] E.R. Jamieson, S.J. Lippard, Chem. Rev. 99 (1999) 2467.
[10] W.S. Bowen, W.E. Hill, J.S. Lodmell, Methods Enzymol. 25 (2001) 344.
[11] M.P. Suh, M.Y. Han, J.H. Lee, K.S. Min, C. Hyeon, J. Am. Chem. Soc. 120 (1998) 3819.
[12] C.E. Yoo, P.S. Chae, J.E. Kim, E.J. Jeong, J. Suh, J. Am. Chem. Soc. 125 (2003) 14580.
[13] A. Bencini, E. Berni, A. Bianchi, C. Giorgi, B. Valtancoli, D.K. Chand, H.J. Schneider, J. Chem. Soc., Dalton Trans. (2003) 793.
[14] S.T. Frey, H.H.J. Sun, N.N. Murphy, K.D. Karlin, Inorg. Chim. Acta 242 (1996) 329.

[15] (a) F.V. Rocha, C.V. Barra, A.E. Mauro, I.Z. Carlos, L. Nauton, M. El Ghozzi, A. Gautier, L. Morel, Eur. J. Inorg. Chem. 25 (2013) 4499;
(b) F. Di Sarra, B. Fresch, R. Bini, G. Saielli, A. Bagno, Eur. J. Inorg. Chem. 15 (2013) 2718.
[16] (a) L. Tan, J. Shen, J. Liu, L. Zeng, L. Jin, C. Weng, Dalton Trans. 41 (2012) 4575;
(b) J. Liu, Li-Feng Tan, Lian-He Jin, F. Luan, DNA Cell Biol. 31 (2012) 250;
(c) L. Jin, L. Tan, X. Zou, J. Liu, F. Luan, Inorg. Chim. Acta 387 (2012) 253.
[17] K.J. Humphreys, A.E. Johnson, K.D. Karlin, S.E. Rokita, J. Biol. Inorg. Chem. 7 (2002) 835.
[18] (a) A. Bencini, M. Di vaira, A.C. Fabretti, D. Gatteschi, C. Zanchini, Inorg. Chem. 23 (1984) 1620.;
(b) A. Bencini, C. Benelli, D. Gatteschi, C. Zanchini, Inorg. Chim. Acta 86 (1984) 169.
[19] Y.-T. Li, C.W. Yan, J.-F. Lou, H.-S. Guan, J. Magn. Magn. Mater. 281 (2004) 68.
[20] Y. Journaux, J. Sletten, O. Kahn, Inorg. Chem. 25 (1986) 439.
[21] (a) Y.-T. Li, Z.-H. Jiang, D.-Z. Liao, S.-P. Yan, S.-L. Ma, X.-Y. Li, G.L. Wang, Polyhedron 12 (1993) 2781;
(b) H. Okawa, Y. Kawahara, M.M.S. Kida, Bull. Chem. Soc. Jpn. 53 (1980) 549;
(c) J.S.R. Richardson, K.A. Thomas, B.H. Rubin, D.C. Richardson, Natl. Acad. Sei. USA, 73(2) (1976) 206.;
(d) S. Gambarotta, A. Arena, C. Florian, P.F. Zanazzi, J. Am. Chem. Soc. 104 (1982) 5082;
(e) F. Arena, C. Floriani, A. Chiesi-Villa, C. Guastini, Inorg. Chem. 25 (1986) 4589.
[22] (a) O. Guillou, P. Bergernt, O. Kahn, E. Bakalbassis, K. Boubekeur, P. Bataol, M. Guillot, Inorg. Chem. 31 (1992) 110;
(b) O. Guillou, O. Kahn, R.L. Oushoorn, K. Boubekeur, P. Batail, Inorg. Chim. Acta 119 (1992) 198.
[23] T. Klabunde, C. Eicken, J.C. Sacchettini, B. Krebs, Nat. Struct. Biol. 5 (1998) 1084.
[24] D.D. Perrin, W.L.F. Armarego, D.R. Perrin, Purification of Laboratory Chemicals, Pergamon Press, Oxford, UK, 1980.
[25] (a) E. Amouyal, A. Homsi, J.C. Chaambron, J.P. Sauvage, J. Chem. Soc., Dalton Trans. (1990) 1841;
(b) J.E. Dickeson, L.A. Summers, Aust. J. Chem. 23 (1970) 1023.
[26] Y. Journaux, J. Sletten, O. Kahn, Inorg. Chem. 24 (1985) 4063.
[27] N. Walker, D. Stuart, Acta Crystallogr., Sect. A 39 (1993) 158.
[28] (a) SMART, Siemens Energy & Automation, Inc., Madison, WI, 1996.;
(b) SAINT Version 4 Software Reference Manual; Siemens Energy & Automation, Inc., Madison, WI, 1996.
[29] G.M. Sheldrick, SADABS Version 2 Multi-Scan Absorption Correction Program University of Göttingen, Germany, 2001.
[30] G.M. Sheldrick, SHELX 97 Programs for Crystal Structure Solution and Refinement, University of Göttingen, Göttingen Germany, 1997.
[31] M.N. Burnett, C.K. Johnson, ORTEP-III Report ORNL-6895, Oak Ridge National Laboratory Oak Ridge TN, 1996.
[32] J. Marmur, J. Mol. Biol. 3 (1961) 208.
[33] M.E. Reichmann, S.A. Rice, C.A. Thomas, P. Doty, J. Am. Chem. Soc. 76 (1954) 3047.
[34] (a) J.D. McGhee, P.H. von Hippel, J. Mol. Biol. 86 (1974) 469;
(b) M.T. Carter, M. Rodriguez, A.J. Bard, J. Am. Chem. Soc. 111 (1989) 8901.
[35] (a) J.-B. LePecq, C. Paoletti, J. Mol. Biol. 27 (1967) 87;
(b) S. Neidle, Nat. Prod. Rep. 18 (2001) 291.
[36] G. Cohen, H. Eisenberg, Biopolymers 8 (1969) 45.
[37] J. Bernadou, G. Pratviel, F. Bennis, M. Girardet, B. Meunier, Biochemistry 28 (1989) 7268.
[38] P.K. Mukherjee, R. Balasubramanian, K. Saha, B.P. Saha, M. Pal, Indian Drugs 32 (1995) 274.
[39] R.N. Jones, A.L. Barry, T.L. Gavan, Washington, J.A.I. Microdilution and macrodilution broth procedures, in: E.H. Lennette, A. Balows, W.J. Jr Hausler, H.J. Shadomy (Eds.), Manual of Clinical Microbiology, American Society for Microbiology, Washington, DC, 1985, p. 972.
[40] (a) C.J. Reed, K.T. Douglas, Biochem. J. 275 (1991) 601;
(b) T. Phillips, I. Haq, A.J.H.M. Meijer, H. Adams, I. Soutar, L. Swanson, M.J. Sykes, J.A. Thomas, Biochemistry 43 (2004) 13657.
[41] (a) A.W. Addison, T.N. Rao, J.V. Reedijk, G.C. Verschoor, J. Chem. Soc., Dalton Trans. (1984) 1349;
(b) S.A. Tysoe, R.J. Morgan, A.D. Baker, T.C. Strekas, J. Phys. Chem. 97 (1993) 1707;
(c) J.M. Kelly, A.B. Tossi, D.J. McConnell, T.C. Strekas, Nucleic Acids Res. 13 (1985) 6017;
(d) I.S. Haworth, A.H. Elcock, J. Freemann, A. Rodger, W.G.J. Richards, J. Biomol. Struct. Dyn. 9 (1991) 23;
(e) C. Hiort, P. Lincoln, B. Norden, J. Am. Chem. Soc. 115 (1993) 3448.
[42] H.M. Berman, P.R. Young, Annu. Rev. Biophys. Bioeng. 10 (1981) 87.
[43] C. Cantor, P.R. Schimmel, Biophysical Chemistry, vol. 2, W.H. Freeman, San Francisco, 1980. p. 398.
[44] K.W. Kohn, M.J. Waring, D. Glaubiger, C.A. Friedman, Cancer Res. 35 (1975) 71.
[45] D.S. Sigman, Biochemistry 29 (1990) 9097.
[46] J.M. Kelly, A.B. Tossi, D.J. McConnel, C. OhUigin, Nucleic Acids Res. 13 (1985) 6017.
[47] M. Lee, A.L. Rhodes, M.D. Wyatt, S. Forrow, J.A. Hartley, Biochemistry 32 (1993) 4237.
[48] (a) S. Satyanarayana, J.C. Dabrowiak, J.B. Chaires, Biochemistry 31 (1992) 9319;
(b) T. Hirohama, Y. Kuranuki, E. Ebina, T. Sugizaki, H. Arii, M. Chikira, P.T. Selvi, M. Palaniandavar, J. Inorg. Biochem. 99 (2005) 1205.
[49] Y. Jin, J.A. Cowan, J. Am. Chem. Soc. 127 (2005) 8408.
[50] L.S. Lerman, J. Mol. Biol. 3 (1961) 18.
[51] I. Bertini, H.B. Gray, S.J. lippard, Jacqueline K. Barton (Eds.), Bioinorganic Chemistry: Metal/Nucleic-acid Interactions, University Science Books, California, 1994, p. 457.
[52] (a) C. Bailly, J.B. Chaires, Bioconjugate Chem. 9 (1998) 513;
(b) M. Coll, C.A. Frederick, A.H.-J. Wang, A. Rich, Porc. Natl. Acad. Sci USA 84 (1987) 8385.
[53] (a) O.I. Aruoma, B. Halliwell, M. Dizdaroglu, J. Biol. Chem. 264 (1989) 13024;
(b) S.M. Klein, G. Cohen, A.I. Cederbaum, Biochemistry 20 (1981) 6006.
[54] S. Inoue, S. Kawanishi, Cancer Res. 47 (1987) 6522.
[55] (a) T.B. Thederahn, M.D. Kuwabara, T.A. Larsen, D.S. Sigman, J. Am. Chem. Soc. 111 (1989) 4941;
(b) O. Zelenko, J. Gallagher, D.S. Sigman, Angew. Chem., Int. Ed. Engl. 36 (1997) 2776;
(c) D.S. Sigman, T.W. Bruice, A. Mazumder, C.L. Sutton, Acc. Chem. Res. 26 (1993) 98;
(d) L.E. Marshall, D.R. Graham, K.A. Reich, D.S. Sigman, Biochemistry 20 (1981) 244.